Journal of Pathology
J Pathol March 2022; **256:** 310–320
Published online 22 December 2021 in Wiley Online Library (wileyonlinelibrary.com) DOI: 10.1002/path.5838

ORIGINAL ARTICLE

B7H3 expression and significance in idiopathic pulmonary fibrosis

Chuling Fang[1,2], Andrew E Rinke[1], Jing Wang[1†], Kevin R Flaherty[3], Sem H Phan[1*] and Tianju Liu[1*]

[1] *Department of Pathology, University of Michigan Medical School, Ann Arbor, MI, USA*
[2] *Department of Hematology and Oncology, International Cancer Center, Shenzhen Key Laboratory, Shenzhen University General Hospital, Shenzhen, PR China*
[3] *Department of Division of Pulmonary/Critical Care Medicine, University of Michigan Medical School, Ann Arbor, MI, USA*

**Correspondence to: T Liu or SH Phan, Department of Pathology, University of Michigan Medical School, 109 Zina Pitcher Place, Ann Arbor, MI 48109-2200, USA. E-mail: tianliu@umich.edu or shphan@umich.edu*

†*Present address:* Xinjiang Key Laboratory of Respiratory Disease Research, Traditional Chinese Medicine Affiliated Hospital of Xinjiang Medical University, Urumqi, 830000, PR China

Abstract

The clinical significance of B7H3 (CD276) and its cleavage product soluble B7H3 (sB7H3) in idiopathic pulmonary fibrosis (IPF) is unknown. Mounting evidence suggests the potential utility of peripheral blood myeloid cell enumeration to predict disease outcome and indicate active lung disease. Here we hypothesized that sB7H3 is involved in regulation of circulating myeloid cells in pulmonary fibrosis. In support of this possibility, both plasma sB7H3 and B7H3$^+$ cells were elevated in IPF patient blood samples, which correlated negatively with lung function. To analyze its function, the effects of sB7H3 on naïve or bleomycin-treated mice were examined. The results revealed that sB7H3 injection induced an influx of myeloid-derived suppressor cells (MDSCs) and *Ccl2* expression in lung tissue of naïve mice, accompanied by enhanced overall inflammation. Additionally, sB7H3 caused accumulation of MDSCs in bone marrow with increased expression of inflammatory cytokines. Notably, *in vitro* assays revealed chemotaxis of MDSCs to sB7H3, which was dependent on TLT-2 (TREML2), a putative receptor for sB7H3. Thus, increased circulating sB7H3 and/or B7H3$^+$ cells in IPF patient blood samples correlated with lung function decline and potential immunosuppressive status. The correlation of sB7H3 with deterioration of lung function might be due to its ability to enhance inflammation and recruitment of MDSCs into the lung and their expansion in the bone marrow, and thus potentially contribute to IPF exacerbation.

Keywords: B7H3; bone marrow; MDSC; cell migration; inflammation; IPF

Received 1 September 2021; Revised 17 November 2021; Accepted 25 November 2021

No conflicts of interest were declared.

Introduction

Idiopathic pulmonary fibrosis (IPF) is a chronic progressive fibroproliferative lung disease of unknown etiology. Although immunosuppressive treatment does not have benefits in clinical studies [1,2], the role of inflammation and immune dysregulation in the pathogenesis of IPF has been highlighted in previous studies [3], and circulating immune populations have the potential to reflect disease outcome [4]. The numbers of neutrophils and macrophages are increased in the lungs of patients with rapidly progressing IPF [5] and correlated with lower % forced vital capacity (FVC) [6,7]. Monocytes and T lymphocytes are activated in the peripheral blood and bronchoalveolar lavage fluid (BALF) of IPF patients [8]. The numbers of monocytes and Tregs in the peripheral blood are also increased and correlated with disease progression. High monocyte counts indicate a higher risk for poor outcomes and are associated with mortality [4,7,9]. These findings suggest that dysregulated immunity may be important in IPF pathogenesis, especially with respect to acute exacerbation and/or rapid progression of disease.

B7H3 has multiple roles in regulation of the immune system [10]. Metalloproteinase-induced cleavage releases a fragment, soluble B7H3 (sB7H3) [11]. In addition to expression on activated T lymphocytes [12], B7H3 is expressed in monocytes, epithelial cells, osteoblasts, and various human and mouse tumor cells [13–16]. A recent study identified triggering receptor expressed on myeloid cells (TREM)-like transcript 2 (TLT-2, TREML2) as a counter-receptor for B7H3, which upon binding activates CD8$^+$ T-cell proliferation and IFNγ production [16]. However, the precise immunologic function of B7H3 is unclear and controversial in some respects. While increased B7H3 or sB7H3 expression plays an immunosuppressive role to promote tumor invasion and metastasis, its role in asthma exacerbation suggests an opposite role consistent with immune/inflammatory system activation [10,17–19]. In rheumatoid arthritis, B7H3 plays

a co-inhibitory role in inflammatory T-cell responses and inversely correlates with disease severity [20], thus highlighting its bifunctional opposing roles in immune regulation. Elevated levels of sB7H3 in BALF from IPF patients portend an increased likelihood of developing acute exacerbation [21]. In mice, pretreatment with a minimally fibrogenic dose of BLM also caused exacerbation upon subsequent full-dose BLM challenge, but not in B7H3-deficient mice. These findings suggest a novel role for B7H3 in the pathophysiology of pulmonary fibrosis [21]. However, the significance and role of B7H3 in IPF remain largely unknown.

Materials and methods

Study approvals

The human studies were approved by the Institutional Review Board of the University of Michigan, and written informed consent was obtained from participants prior to inclusion in the study. All mice were housed in the University Laboratory Animal Facility in accordance with animal protocols approved by the Institutional Animal Care & Use Committee at the University of Michigan.

Human subjects

Peripheral blood samples were obtained from 65 IPF patients (50 males aged 68.3 ± 6 years, 15 females aged 69.3 ± 6 years) at the University of Michigan between April 2018 and February 2020. The diagnosis of IPF was in accordance with the IPF guidelines [22]. Peripheral blood from ten control subjects was also collected and the age of these controls ranged from 45 to 71 years (2 males and 8 females, aged 61 ± 5 years). Human peripheral blood leukocytes were collected after red blood cell lysis using RBC Lysis Buffer (Cat. # 00-4300-54; eBioscience Inc, San Diego, CA, USA). Freshly isolated cells were resuspended in flow cytometry staining buffer (FACS; 1% BSA in PBS buffer) and then used for flow cytometry analysis on the same day for both total leukocytes.

Mice

C57BL/6J female mice (6 to 8 weeks old) were purchased from The Jackson Laboratory (Bar Harbor, ME, USA). Endotracheal bleomycin (BLM) and/or intravenous (via tail vein) sB7H3 treatments were used for the *in vivo* fibrosis model with/without sB7H3 treatment as indicated. For the *in vivo* treatment with recombinant mouse sB7H3 (# 1397-B3-050/CF; R&D Systems, Minneapolis, MN, USA), 150 and 75 μg/kg (or two doses of 100 μg/kg, respectively) sB7H3 was injected through the tail vein on day 0 and day 2. Control mice received the same volume of PBS alone. The mice were euthanized on day 3 or day 21 for analysis of lung tissues and cells. To evaluate the effects of sB7H3 on BLM-induced fibrosis, mice were treated with BLM (Mead Johnson, Princeton, NJ, USA) dissolved in sterile PBS by endotracheal instillation at a dose of 2.25 U/kg body weight on day 0. Then 100 μg/kg sB7H3 was injected through the tail vein on days 12, 14, and 16. Control mice received the same volume of PBS alone. The mice were euthanized on day 21 and the lungs and bone marrow (BM) were harvested for analysis by flow cytometry and RT-qPCR analysis. Peripheral blood was also collected for flow cytometry analysis. The right lungs were collected for total RNA isolation and single cell suspensions. Paraffin-embedded left lung sections were stained with H&E or Masson's trichrome for evaluation of histopathology.

Cell isolation and treatment

Lung tissue single cell suspensions and BM cells for flow cytometry were isolated as described previously [23]. Mouse lung fibroblasts obtained from single cell suspension were maintained in DMEM supplemented with 10% plasma-derived fetal bovine serum (PDS; Animal Technologies, Tyler, TX, USA), 10 ng/ml EGF, and 5 ng/ml PDGF (R&D Systems) as before. Lung fibroblasts at passages 1–5 were used in the indicated experiments. Where indicated, the cells were treated with 5 ng/ml TGFβ for 24 h. For BM cell *in vitro* experiments, $CD11b^{+}Gr1^{+}$ myeloid-derived suppressor cells (MDSCs) were isolated from BMs using the EasySep™ Mouse Myeloid-Derived Suppressor Cell Isolation Kit (# 19867; STEMCELL Technologies, Cambridge, MA, USA) according to the manufacturer's instructions. $F4/80^{+}$ cells were isolated from BMs using an anti-F4/80 microbeads ultrapure kit (# 130-110-443) and separation column (# 130-042-401; Miltenyi Biotec, Bergisch Gladbach, Germany). Freshly isolated cells were treated with sB7H3 at the indicated doses and time points.

BM cell *in vitro* experiment

Whole BM cells from naïve mice were maintained in RPMI-1640 (# 11875-093; Thermo Fisher Scientific, Waltham, MA, USA) containing 10% fetal bovine serum (Sigma, St Louis, MO, USA) for 24 h, and starved with 1% serum for another 24 h before the indicated treatments. The cells were treated with 1, 2 or 5 μg/ml sB7H3 (# 1397-B3-050; R&D Systems) for 4, 6 or 24 h, as indicated; $F4/80^{+}$ BM cells were treated with 5 μg/ml sB7H3 for 4 h, and then cells were harvested for RT-qPCR analysis. All cells in each group were plated on six-well plates with 4×10^{6} cells in each well. Whole BM cells from naïve mice were treated also with 2 μg/ml sB7H3 for 3 days and then harvested for flow cytometry analysis.

Cell migration assays

Migration assays of BM cells or MDSCs were performed in Corning 24-well Transwell plates with 3-μm pore size polycarbonate filters (# 3415; Corning, New York, NY, USA). Cells were pre-labeled with 5 μM Calcein AM (# 564061; BD Biosciences, San José, CA, USA) for 30 min

at 37 °C, 5% CO_2. Following incubation, cells were washed twice and resuspended in serum-free RPMI-1640 at a density of 1×10^6 cells per 100 µl. Serum-free RPMI-1640 medium (600 µl) or medium containing sB7H3 (5 µg/ml) was placed in the lower chamber and 1×10^6 per 100 µl labeled cells were loaded onto each upper chamber. Cell migration to the lower chambers was determined at various time points (1, 4, and 18 h) by measuring the fluorescence intensity at 485/530 nm (Ex/Em) using a SpectraMax Gemini EM Microplate Reader (Molecular Devices, San José, CA, USA). The intensities measured at different times were corrected for the average of their respective controls (buffer only). The number of migrated cells in the lower chamber was also counted under the microscope. Where indicated, the Calcein AM-stained MDSCs were incubated with anti-mouse TREML2 (TLT-2) monoclonal antibody (15 µg per 1×10^6 cells) (# MA5-24295, clone 656906; Thermo Fisher Scientific) or IgG2a isotype control (15 µg per 1×10^6 cells) (# 02-9688; Thermo Fisher Scientific) for 1 h prior to placing into the upper chambers.

The checkerboard assay to confirm chemotaxis was performed using Corning® FluoroBlok™ 96-Multiwell Insert Plates with 3.0 µm High Density PET Membrane (# 351161; Thermo Fisher Scientific). Calcein AM pre-stained MDSCs (1×10^5 per 50 µl) were seeded in the upper chamber. Increasing concentrations of sB7H3 (0, 5, 10, and 15 µg/ml) were added to the upper or lower chamber of the plates, as indicated. The plates were incubated for 18 h followed by fluorescence measurement to count the migrated cells.

Flow cytometry

Single cell suspensions from mouse BM, lung or peripheral blood were prepared for flow analysis and analyzed as before [21]. Antibodies (and fluorophores) for mouse samples used in this study were as follows: lineage-APC cocktail of anti-CD3e, CD11b, B220, Ly-76, Ly-6C, Ly-6G (# 558074, dilution 1:5; BD Biosciences); CD11b-AmCyan (# 101263, clone M1/70, dilution 1:20), Ly6C-FITC (# 128006, clone HK1.4, dilution 1:200), Ly6G-BV421 (# 127628, clone 1A8, dilution 1:20), F4/80-APC-Cy7 (# 123118, clone BM8, dilution 1:20), F4/80-APC (# 123116, clone BM8, dilution 1:100), CD206-PE-Cy7 (# 141719, clone C068C2, dilution 1:100), CCR2-PE (# 150610, clone SA203G11, dilution 1:50), CD86-APC-Cy7 (# 105030, clone GL-1, dilution 1:100; all BioLegend, San Diego, CA, USA). Human whole blood cells were stained with B7H3-PE (# 331606, clone DCN.70, dilution 1:20; BioLegend). Both mouse and human cells were also stained with isotype controls conjugated with the same fluorochrome as their respective antibodies and each single-color antibody that was included in the antibody mixes. The data were then acquired using a NovoCyte flow cytometer and analyzed using NovoExpress software (Acea Biosciences, Inc, San Diego, CA, USA). Monocytic MDSCs (M-MDSCs) were defined as $CD11b^+Ly6C^{hi}Ly6G^-$ and granulocytic MDSCs (G-MDSCs) were defined as $CD11b^+Ly6C^{low/-}Ly6G^+$. Myeloid-derived macrophages were defined as $CD11b^+F4/80^+$. Type 1 macrophages (M1) were defined as $CD11b^+F4/80^+CD206^-CD86^+$ and type 2 macrophages (M2) as $CD11b^+F4/80^+CD206^+$.

RT-qPCR

RNA extraction and RT-qPCR for lung tissue or BM cells were performed as described previously [24]. Taqman probes for mouse B7H3 (*Cd276*) (Mm00506020_m1), *Tnfa* (Mm00443258_m1), *Il1b* (Mm00434228_m1), *Arg1* (Mm00475988_m1), *Nos2* (Mm00440502_m1), *Ccr2* (Mm04207877_m1), *Ccl2* (Mm00441242_m1), *Gmcsf* (Mm01290062_m1), *Col1a2* (Mm00483888_m1), and 18S rRNA (# 4352655) were purchased from Thermo Fisher Scientific. One hundred nanograms of total RNA was used for Taqman qPCR. The mRNA levels were expressed relative to the internal control (18S rRNA) and normalized to the indicated control group (equaled 1), and expressed as $2^{-\Delta\Delta CT}$ as described previously [25].

ELISA assay

The levels of sB7H3 in human or mouse plasma samples were measured using ELISA kits from R&D Systems or LifeSpan BioSciences, Inc (Seattle, WA, USA), respectively, in accordance with the manufacturer's protocols.

Statistics

All experiments were performed two or three times, and representative data or pooled data are shown as mean ± SD. Differences between any two groups were assessed for statistical significance using Student's *t*-test or ANOVA with Fisher's LSD *post hoc* comparison test in multiple group comparison. Where indicated, the statistical analyses were also performed using GraphPad Prism 8.2.1 (GraphPad Software Inc, San Diego, CA, USA). All correlation coefficients for parameters were calculated using Pearson correlation coefficient analysis. *P* values less than 0.05 were considered statistically significant.

Results

Induction of B7H3 in BLM-induced fibrosis mouse and IPF patients

Analysis by ELISA revealed a significant increase in sB7H3 in plasma samples from IPF patients compared with those from healthy subjects (mean of 14.7 versus 9.7 ng/ml) (Figure 1A). We measured the number of $B7H3^+$ cells in peripheral blood of IPF patients and analyzed further for a possible association with the levels of plasma sB7H3. The results showed that although the increased percentage of circulating $B7H3^+$ cells in IPF patient samples compared with normal controls was not statistically significant (0.114 versus 0.236%, $p = 0.136$, Figure 1B), there was a significant positive correlation between plasma sB7H3 levels and $B7H3^+$

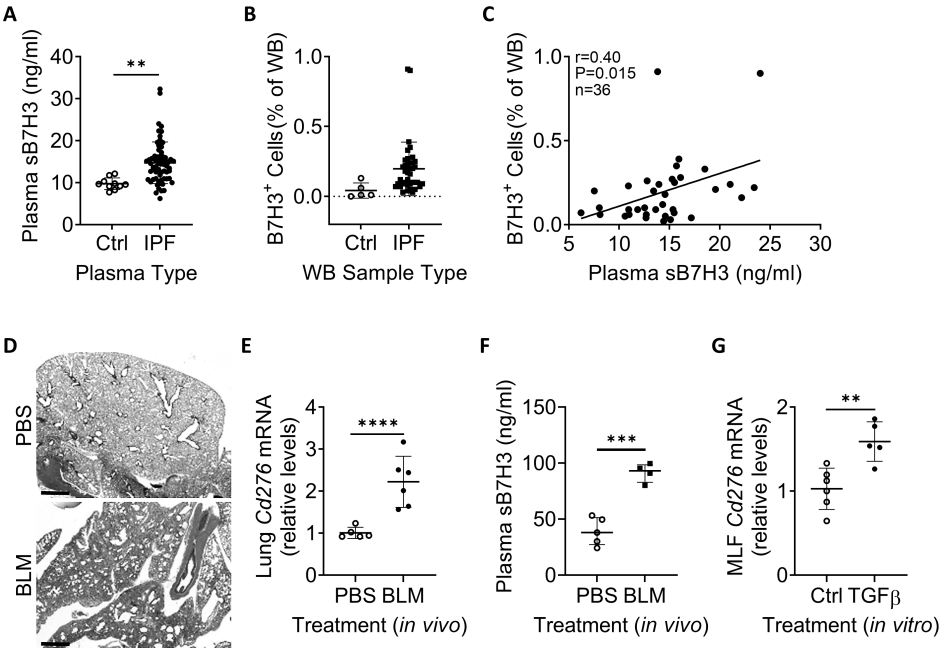

Figure 1. B7H3 in human IPF and BLM-induced mouse lung fibrosis. (A) Levels of sB7H3 in plasma samples from IPF patients ($N = 65$) and healthy controls (Ctrl, $N = 10$) were measured by ELISA. (B) Abundance of B7H3$^+$ cells in peripheral white blood cells (WB) of IPF patients analyzed by flow cytometry. $N = 5$ for Ctrl and 39 for IPF. (C) Correlation between plasma sB7H3 level and B7H3$^+$ cells from WB of IPF patients. $N = 36$. $p < 0.05$. (D) Representative mouse lung tissue sections at 21 days after BLM treatment were stained using H&E. Scale bar: 1 mm. (E) The level of B7H3 mRNA (*Cd276*) in lung tissues on day 21 after BLM treatment. 18S rRNA was used as an internal control. The results were calculated as $2^{-\Delta\Delta CT}$ and are expressed as fold-change relative to the controls. $N = 6$ mice per group. (F) Levels of sB7H3 in plasma samples from PBS or BLM-treated mice on day 21 ($N = 5$ in PBS, 4 mice in BLM groups) were measured by ELISA. (G) The expression of *Cd276* in TGFβ-treated mouse lung fibroblasts (MLF). $N = 5$ for control and 6 for TGFβ-treated cells. Ct values for *Cd276* in lung tissue or fibroblasts: ~24–26. $^{**}p < 0.01$, $^{***}p < 0.001$, $^{****}p < 0.0001$.

cell abundance in IPF patient blood samples (Figure 1C). This correlation and significance were similar even after removing two apparent 'outliers' ($r = -0.38$, $p = 0.027$). In mice, while BLM induced significant injury as seen in lung tissue sections by histology examination (Figure 1D), *Cd276* was significantly elevated by more than two-fold in the lung tissue on day 21 of BLM-treated mice compared with control mice (Figure 1E). Consistent with the induction of its mRNA expression, sB7H3 protein level was significantly increased in mouse plasma samples 21 days after BLM treatment (Figure 1F). *In vitro*, *Cd276* was also induced in TGFβ-treated mouse lung fibroblasts after 24 h of treatment (Figure 1G). These observations indicated that both *Cd276* and protein levels were induced in both IPF and mouse lung fibrosis.

sB7H3 levels or B7H3$^+$ cell abundance correlated with lung function in IPF patients

To assess clinical significance, we analyzed for a possible association between plasma sB7H3 level or B7H3$^+$ cell abundance in whole blood and lung function. By Pearson correlation analysis, we found that the plasma sB7H3 was inversely correlated with carbon monoxide diffusion capacity (DLCO, % predicted) (Figure 2A). Furthermore, the percentage of B7H3$^+$ cells significantly correlated with lower DLCO, but the correlation became insignificant ($p = 0.071$) when two 'outlier' data points (B7H3$^+$ cells > 0.8%) were excluded, although a similar correlation trend ($r = 0.32$) was observed (Figure 2B). These findings indicated that the level of sB7H3 and the abundance of circulating B7H3$^+$ cells in peripheral blood may reflect disease progression and/or severity in IPF patients.

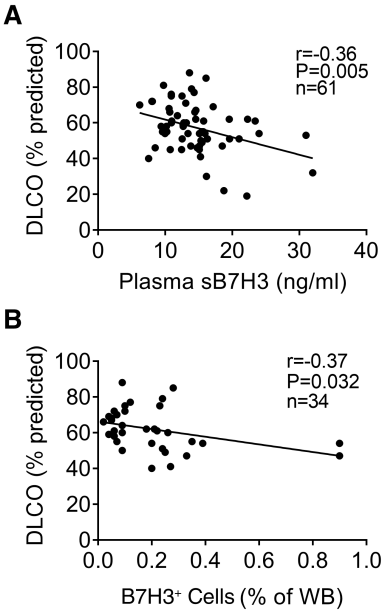

Figure 2. B7H3 and lung function. Linear regression analysis (A) of plasma sB7H3 versus DLCO from all IPF patients ($N = 61$), $p < 0.01$, and (B) between B7H3$^+$ cells in peripheral white blood cells (WB) and DLCO from all IPF patients ($N = 34$). $p < 0.05$.

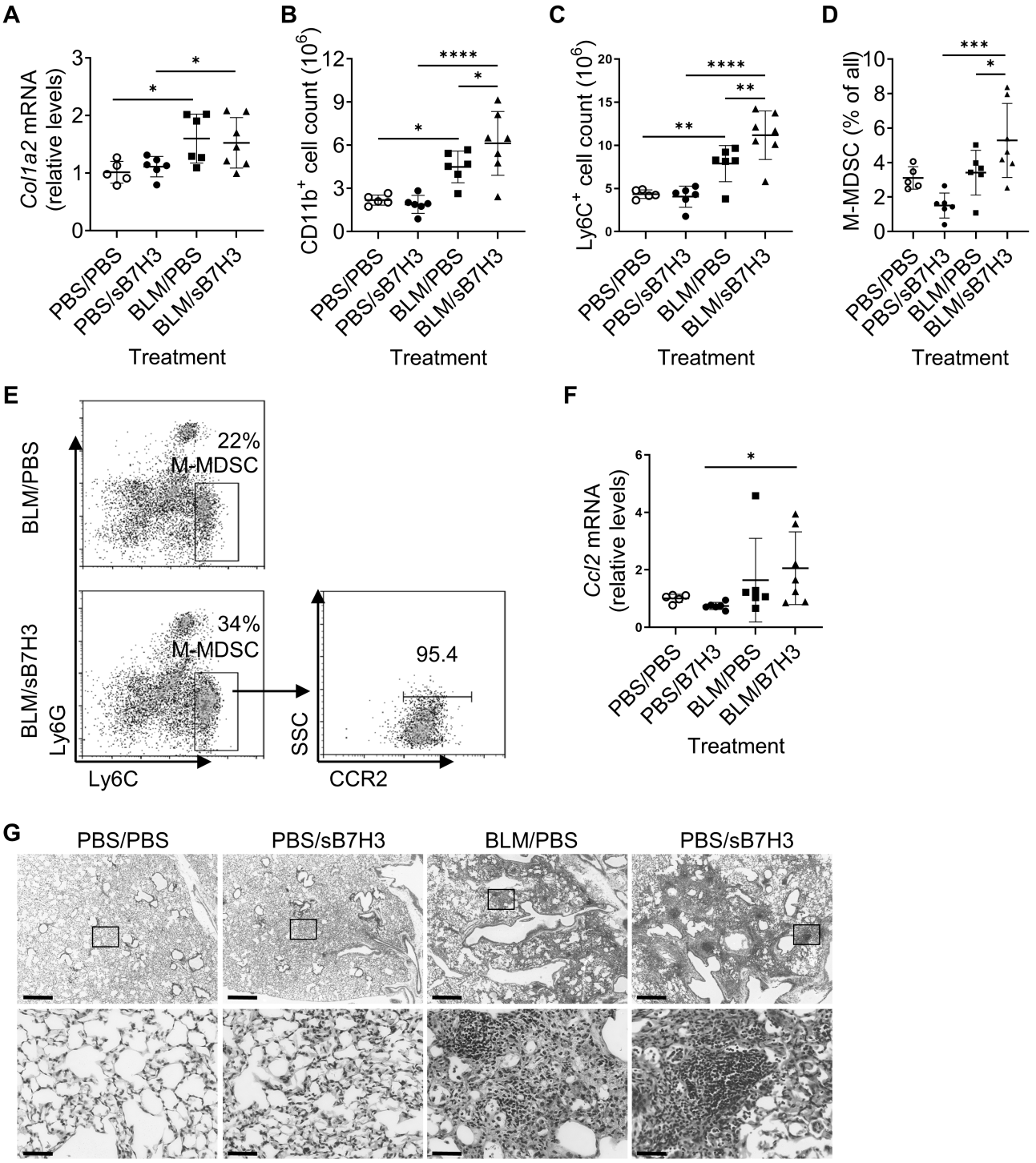

Figure 3. Effects of delayed sB7H3 treatment on the mouse BLM model. Mice were treated with BLM endotracheally on day 0 and then received three doses of sB7H3 injections on days 12, 14, and 16 via the tail vein. The mice were euthanized on day 21 for analysis as follows: (A) type I procollagen mRNA (*Col1a2*) in the lung was assessed using RT-qPCR; (B) lung CD11b$^+$ and (C) Ly6C$^+$ cells were analyzed by flow cytometry, and their cell numbers in whole lung tissue are shown. (D) The percentages of M-MDSCs in whole lung single suspensions were quantified using flow cytometry analysis. (E) The MDSCs in the lung single cell suspensions (pooled from every two mice) in the BLM and BLM + sB7H3 groups were analyzed by flow cytometry. Representative plots for MDSC and CCR2$^+$ populations are shown with average number of percentages. (F) Lung *Ccl2* mRNA (for MCP1) was analyzed as described in A. (G) Representative lung tissue sections were stained using H&E. Scale bars: 50 μm. The high-power (×400) images were taken from the areas boxed in the top panel images. $N = 5$–7 mice per group for all. In A–D, and F, the data points represent individual animals. *$p < 0.05$, **$p < 0.01$, ***$p < 0.001$.

sB7H3 facilitated recruitment of MDSCs and lung inflammatory response in murine pulmonary fibrosis

Since plasma sB7H3 correlated inversely with lung function in IPF patients (Figure 2A), we explored whether sB7H3 could enhance the BLM-induced lung inflammation and/or fibrosis, or potentially trigger the disease exacerbation occurring after fibrosis developed in mice. The results showed that sB7H3 treatment

commencing on day 14 after BLM treatment did not significantly affect the BLM-induced collagen I (*Col1a2*) expression, although BLM treatment caused significant *Col1a2* induction at the mRNA level compared with their respective control groups with or without sB7H3 treatment (Figure 3A). However, BLM-induced $CD11b^+$ and $Ly6C^+$ cell numbers were enhanced by sB7H3 treatment (Figure 3B,C), indicating that delayed sB7H3 treatment was associated with increased heightened level of inflammation and/or its persistence. We further investigated the role of B7H3 in immune cells in response to BLM injury. While BLM treatment alone had no significant effect on the abundance of lung $CD11b^+Ly6C^{hi}Ly6G^-$ monocytic MDSCs (M-MDSCs), additional delayed treatment with sB7H3 revealed a significantly elevated number of these cells in the lung (Figure 3D), but not $CD11b^+Ly6C^{lo/-}Ly6G^+$ granulocytic MDSCs (G-MDSCs) (data not shown). Among the induced lung M-MDSCs, more than 95% were positive for CCR2 (Figure 3E). Interestingly, mice treated with BLM plus sB7H3 also exhibited significantly higher levels of lung *Ccl2* mRNA (Figure 3F). Histopathological analysis showed a higher inflammatory cell density in the lung tissue sections from sB7H3-injected mice compared with the PBS group. Moreover, the lung tissue sections from the BLM/sB7H3 groups showed denser inflammatory cell infiltration with multiple lymphoid cell clusters and severe distortion of the lung architecture compared with their corresponding controls (BLM/PBS). Consistent with the changes in *Col1a2* mRNA, similar fibrotic lesions were displayed in lung tissue sections between the BLM/PBS and BLM/sB7H3 groups (Figure 3G). Fibrosis was also confirmed using Masson's trichrome staining for collagen deposition in the lung interstitium (supplementary material, Figure S1). These findings suggested that delayed sB7H3 injections caused enhanced inflammation along with an increased influx of BM-derived $Ly6C^+$ inflammatory cells as well as MDSCs in the BLM-injured lung.

Effects of sB7H3 on inflammatory cell types *in vitro* and *in vivo*

BM-derived myeloid cells and sB7H3-induced expansion of BM $Ly6C^{hi}$ monocytic cells are suspected of playing a significant role in IPF, especially in acute exacerbation [21,23,26]. Further analysis by flow cytometry (Figure 4A) revealed that sB7H3 significantly induced both $Ly6G^+$ and $Ly6C^+$ cells in this $CD11b^+$ myeloid population (Figure 4B). Among these significantly induced populations were $CD11b^+Ly6C^{lo/-}Ly6G^+$G-MDSCs and $CD11b^+Ly6C^{hi}Ly6G^-$ M-MDSCs (Figure 4C).

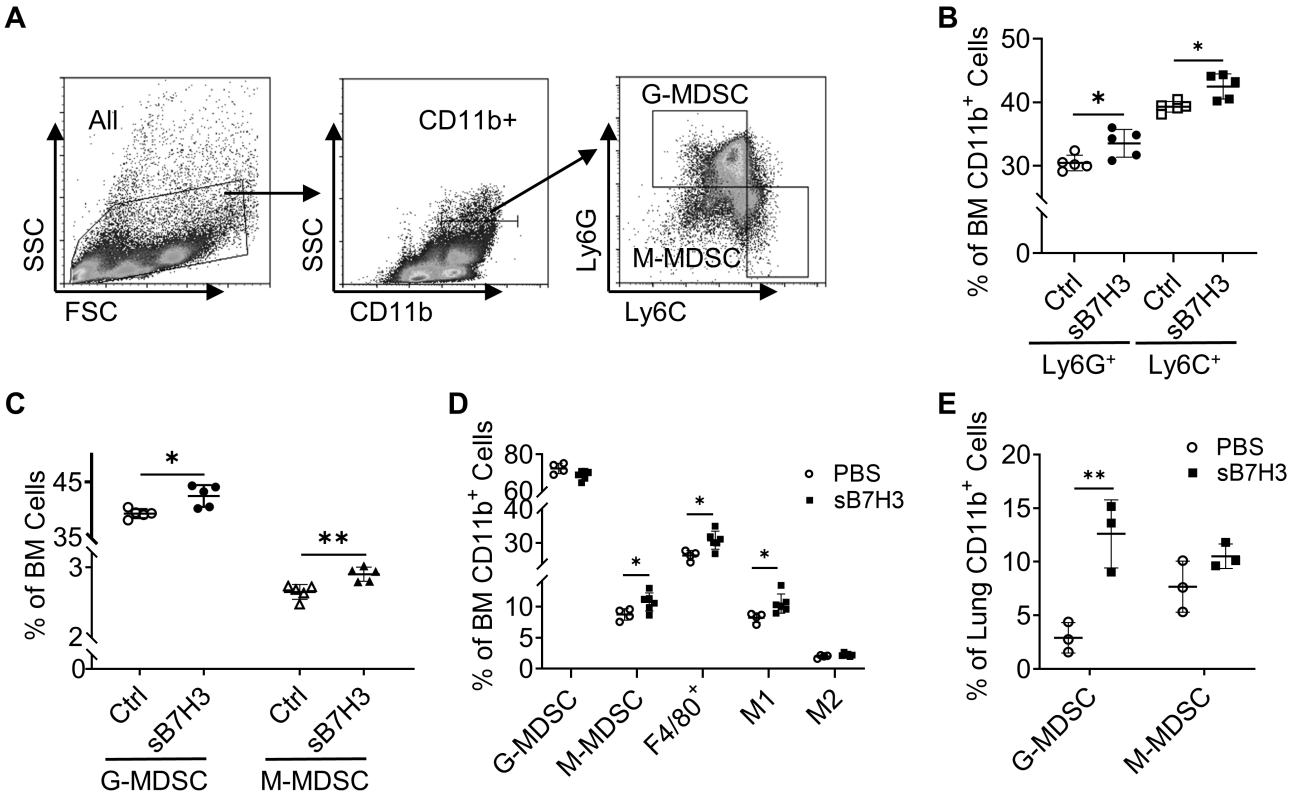

Figure 4. *In vitro* and *in vivo* effects of sB7H3 on myeloid cells. (A) Characterization and flow gating strategy of MDSCs in mouse BM cells. G-MDSCs were defined as $CD11b^+Ly6G^+Ly6C^{lo/-}$ cells and M-MDSCs as $CD11b^+Ly6C^{hi}Ly6G^-$ cells. (B) Effects of sB7H3 on $Ly6G^+$ and $Ly6C^+$ cells in the BM $CD11b^+$ population. $N = 5$ per group. (C) Effects of sB7H3 on G-MDSCs and M-MDSCs isolated from whole BM cells. $N = 5$ per group. (D) Three days after PBS or sB7H3 injection, BM cells were harvested and analyzed for MDSCs and $F4/80^+$, M1 and M2 macrophages by flow cytometry. Results are expressed as percent of the total BM $CD11b^+$ population. $N = 4$ in control and 6 mice in sB7H3-treated groups. (E) On day 21 after treatment with PBS or sB7H3, the lungs were harvested and analyzed for MDSCs using flow cytometry. The results are expressed as percent of lung $CD11b^+$ cells. $N = 3$ mice per group. ANOVA with Tukey's multiple comparisons test. $^*p < 0.05$, $^{**}p < 0.01$.

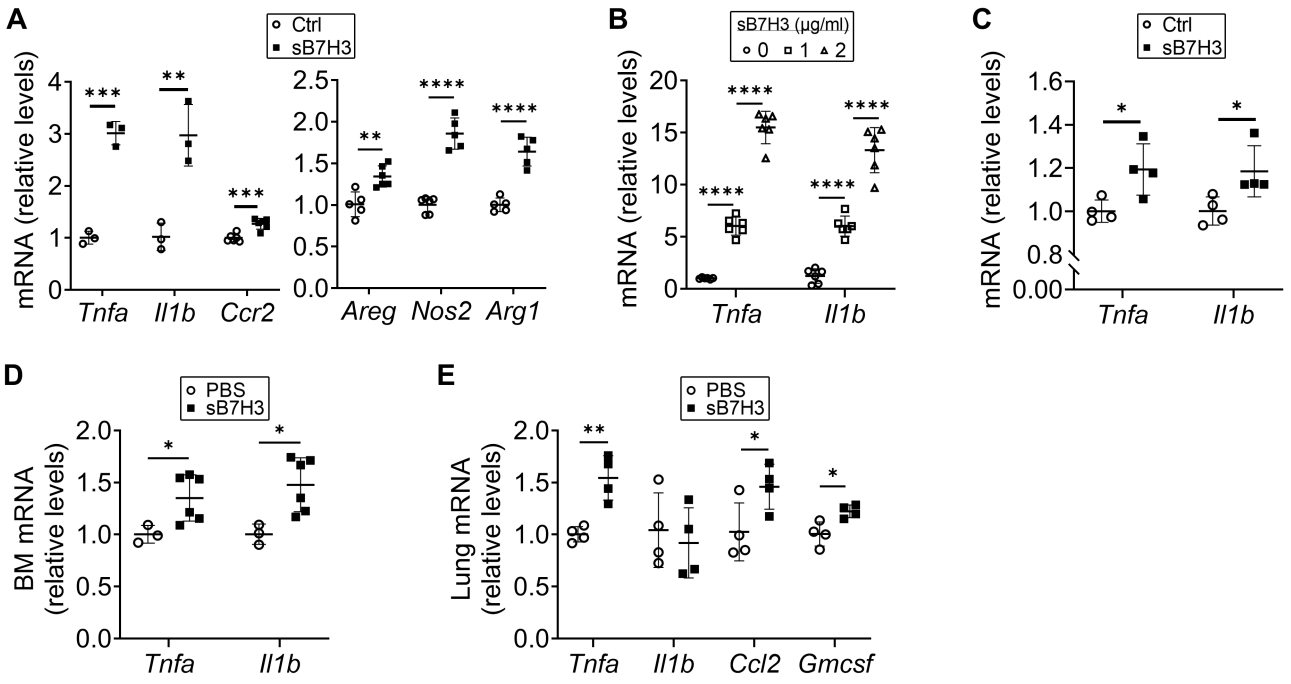

Figure 5. Induction of inflammatory cytokines/chemokines by sB7H3 *in vitro* and *in vivo*. (A) BM cells isolated from naïve mice were treated with sB7H3 (2 μg/ml) and then analyzed by RT-qPCR for expression of *Tnfa*, *Il1b*, and *Ccr2* ($N = 3$–6 mice per group), as well as *Nos2*, *Areg*, and *Arg1* 4 h after treatment ($N = 5$–6 mice per group). (B) Expression of *Tnfa* and *Il1b* in response to sB7H3 treatment at 4 h ($N = 6$ per group). (C) $CD11b^+F4/80^+$ cells isolated from BM were treated with sB7H3 for 4 h and then analyzed for the expression of *Tnfa* and *Il1b* ($N = 4$ per group). (D) RT-qPCR analysis was performed for the indicated BM mRNAs on day 3 after sB7H3 single dose injection in mice. $N = 3$ in PBS control and 6 mice in sB7H3 injected group. (E) The indicated lung tissue mRNAs on day 21 after sB7H3 injection were analyzed by RT-qPCR. $N = 4$ mice per group. $^*p < 0.05$, $^{**}p < 0.01$, $^{***}p < 0.001$, $^{****}p < 0.0001$.

We next investigated the effects of sB7H3 *in vivo*. Since sB7H3 changed the percentages of MDSCs *in vitro*, we mainly focused on possible direct effects of sB7H3 on MDSCs and myeloid-derived macrophages. *In vivo* studies revealed that sB7H3 induced M-MDSCs, $CD11b^+F4/80^+$ cells, and M1 macrophages ($CD11b^+F4/80^+CD86^+CD206^-$) in mouse BM $CD11b^+$ cells on day 3 (Figure 4D), indicating an ability to activate/mobilize BM myeloid-derived populations. However, on day 21 after sB7H3 injection, the BM had reverted back to normal (data not shown), while the percentages of G-MDSCs and M-MDSCs in the lung were increased but significantly only for the former (Figure 4E).

Effects of sB7H3 on inflammatory cytokines

In addition to the effects on myeloid cell differentiation, we explored the effects of sB7H3 on the expression of mRNAs for inflammatory cytokines in BM cells. The results showed that sB7H3 significantly increased the expression of *Tnfa*, *Il1b*, *Ccr2*, *Areg* (amphiregulin), *Nos2*, and *Arg1* in BM cells 4 h after treatment (Figure 5A). Moreover, the effect of sB7H3 on *Tnfa* and *Il1b* mRNAs was dose-dependent (Figure 5B). Our analysis of the effects of sB7H3 on BM $CD11b^+F4/80^+$ cells and MDSCs revealed that sB7H3 significantly increased the expression of *Tnfa* and *Il1b* in the $F4/80^+$ BM cells only (Figure 5C; not shown for MDSCs). *In vivo* sB7H3 also significantly increased the expression of *Tnfa* and *Il1b* in BM cells 3 days after treatment (Figure 5D). Furthermore, this *in vivo* treatment also induced the expression of *Tnfa*, *Ccl2*, and *Gmcsf*, but not *Il1b*, in lung tissue at day 21 after treatment (Figure 5E). These findings suggested that sB7H3 was capable of directly inducing BM inflammatory cytokines/chemokines of potential pathophysiological relevance *in vivo*.

sB7H3 increased the migration of inflammatory cells through chemotaxis and this effect might depend on TLT-2

To evaluate the possible mechanism by which B7H3 induced a further increase in the number of MDSCs and overall inflammation in the BLM-injured lung, we investigated the effect of sB7H3 on BM cell migration. The results showed that sB7H3 caused significantly increased migration of BM cells in a time-dependent manner up to 18 h of incubation (Figure 6A). This result was confirmed by direct cell counting of the absolute number of migrated cells in each lower chamber (Figure 6B). The same results were observed with isolated BM $Ly6C^+$ or $Ly6G^+$ cells (data not shown). Stimulation of migration by sB7H3 was also observed in MDSCs isolated from BM cells (Figure 6C). A checkerboard assay confirmed that increased MDSC migration was dependent on the concentration of sB7H3 in the bottom chamber but not in the upper chamber, indicating that chemotaxis (rather than chemokinesis) was the basis for the sB7H3-induced cell migration (Figure 6D).

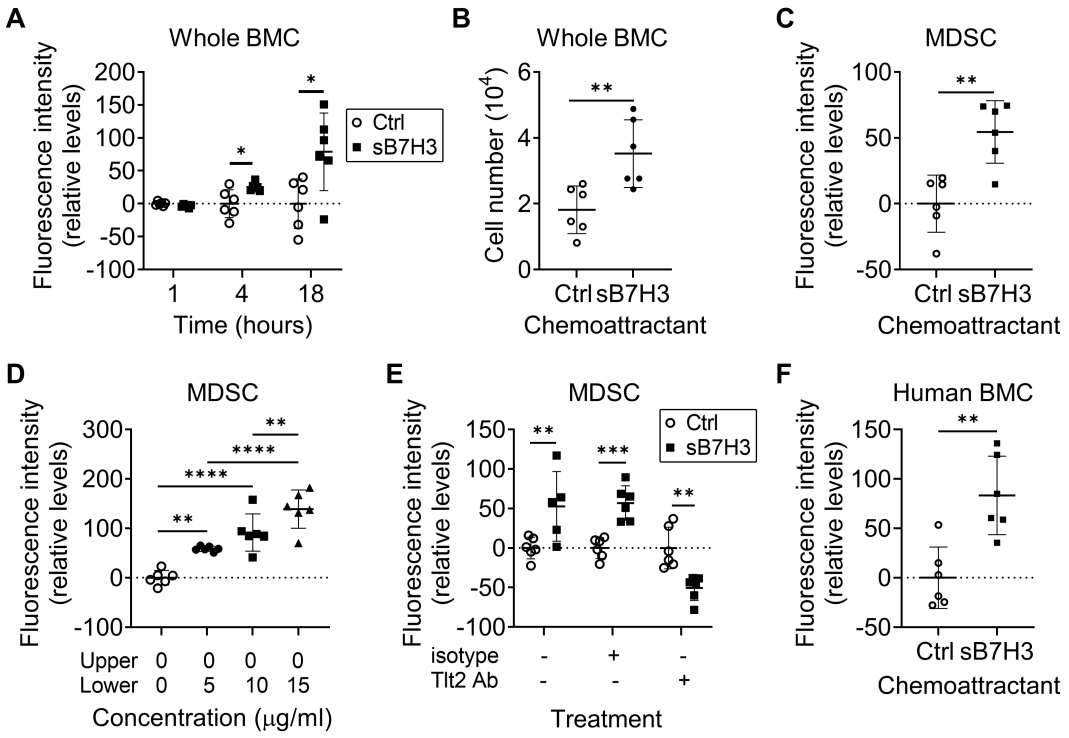

Figure 6. Effects of sB7H3 on mouse and human myeloid cell migration. (A) Freshly isolated BM cells pre-labeled with Calcein AM were placed in the upper chamber, while buffer or sB7H3-containing media were placed in the bottom chamber. The fluorescence intensity of the lower chamber with migrating cells was monitored after 1, 4 or 18 h of incubation. The intensities measured at different time points were normalized to the average of their respective controls (buffer only). (B) The migrated cells in the lower chambers at 18 h after incubation were also counted using a microscope, and the absolute cell numbers are shown. $N = 6$ per group. (C) Pre-labeled MDSCs isolated from naïve BM were placed in the upper chamber, and the fluorescence intensity of the lower chamber was measured after 4 h of incubation. (D) A checkerboard assay was carried out as described in the legend for Table 1. The data from four groups in the absence of sB7H3 in the upper chamber are shown. $N = 6$ per group. (E) Similarly isolated and pre-stained BM MDSCs were pre-incubated with an antibody to TLT-2 (TREML2) or an isotype control for 1 h prior to being placed in the upper chambers and then incubated in the presence or absence of sB7H3 in the lower chambers. The fluorescence intensity was measured 4 h later. The intensities of different wells were normalized to the average of their respective controls in different pretreatment groups. $N = 6$ per group. (F) Human BM mononuclear cells were placed in the upper chamber, and the fluorescence intensity of the lower chamber was measured after 4 h of incubation. $N = 6$ per group. $^*p < 0.05$, $^{**}p < 0.01$, $^{***}p < 0.001$, $^{****}p < 0.0001$.

TLT-2 (TREML2) has been suggested as a putative B7H3 receptor [16]. To determine if TLT-2 is essential for the chemotactic activity of sB7H3, we examined the impact of neutralizing antibodies against TLT-2 on MDSC migration. The effect of sB7H3 on MDSC migration was completely abolished when TLT-2 on these cells was blocked by the antibodies (Figure 6E), suggesting that TLT-2 was essential in mediating the chemotactic activity of sB7H3. Finally, to assess potential clinical relevance, human BM mononuclear cells were used as the target cells in the same migration assay. Consistently, human sB7H3 was also able to significantly induce human BM mononuclear cell migration (Figure 6F). These findings suggested a potentially significant role for sB7H3 in chemotactic recruitment of BM myeloid cells in response to lung injury and exacerbation of fibrosis.

Discussion

In this study, we investigated the significance of B7H3 expression in pulmonary fibrosis based on previous observation of its potential role in exacerbation of IPF [21]. First, we demonstrated that the plasma level of

Table 1. Checkerboard analysis of the effects of sB7H3 (μg/ml) on BM MDSC migration

	sB7H3 (upper)			
	0	5	10	15
sB7H3 (lower)				
0	211.43 ± 14.84	221.00 ± 14.08	247.75 ± 13.57	186.740 ± 17.48
5	270.10 ± 5.03	264.43 ± 8.83	287.84 ± 23.39	217.78 ± 9.62
10	302.94 ± 37.53	287.73 ± 47.74	347.57 ± 22.43	208.07 ± 31.15
15	350.28 ± 38.69	298.72 ± 45.23	331.16 ± 23.64	236.01 ± 20.90

$CD11b^+Gr1^+$ MDSCs were isolated from BM of naïve mice and used in a chemotaxis assay after labeling with a fluorescence tag. The cells were placed in the upper chamber with increasing concentrations of sB7H3 in the upper and lower chambers as indicated in the table. Values are fluorescence intensities of migrated cells found in the lower chambers after incubation for 18 h. Mean ± SD. $N = 6$ per group.

sB7H3 and the percentage of circulating $B7H3^+$ cells in peripheral blood were increased in patients with IPF when compared with healthy controls, which suggested potential significance in pathogenesis. More importantly, higher levels of plasma sB7H3 or peripheral blood $B7H3^+$ cells correlated significantly with worse lung function (DLCO). This further suggests their potential utility as biomarkers for disease progression and/or response to therapy. In addition, levels of plasma sB7H3 closely correlated with the abundance of $B7H3^+$ cells, suggesting these cells as a potential source of sB7H3, consistent with a previous study showing its derivation by cleavage from membrane-bound B7H3 [11]. The released sB7H3 could then play a role in the recruitment of BM myeloid cells, such as the noted MDSCs and $Ly6G^+/Ly6C^+$ inflammatory cells, as well as promote the differentiation of these cells toward an M1 phenotype with elaboration of pro-inflammatory cytokines, thus potentially causing or contributing to IPF exacerbation.

The functional role of B7H3 is controversial, having been reported to provide either positive or negative co-stimulatory signals [20,27]. The findings in our study appear to be consistent with a potentially immunosuppressive role by increasing the abundance of MDSCs, perhaps in part due to the release of sB7H3 and consequent chemotactic recruitment. However, the effects on BM myeloid cell differentiation suggest a pro-inflammatory activity. To seek out potential mechanisms, we examined the effects of sB7H3 alone, and in the BLM-induced model of lung injury and fibrosis, as well as on isolated BM cells *in vitro*. In the BLM-induced fibrosis mouse model, sB7H3 injection enhanced lung inflammation at a late time-point when the inflammation due to BLM-induced injury alone is known to have waned [28,29]. This enhanced inflammation could be attributable to sB7H3 inhibition of the turn-off signal, resulting in persistence of the innate immune response in addition to, or instead of, solely enhancing it. Furthermore, sB7H3 increased the percentage of MDSCs in the BM initially, followed by an increase in the lungs. This time sequence would suggest a role for sB7H3 in myeloid cell differentiation and recruitment from the BM, which would be consistent with its documented TLT-2-dependent chemotactic activity. In BM, cell differentiation induced by sB7H3 was characterized by the elevated expression of pro-inflammatory cytokine mRNAs (*Tnfa* and *Il1b*), suggesting an M1 cell phenotype. Similarly, in a mouse model of experimental pneumococcal meningitis, B7H3 treatment increased the levels of pro-inflammatory cytokines and chemokines (TNFα, IL1β, IL6, and CCL2) via MAPK p38 and NF-κB p65 pathways [30]. In patients with renal cell carcinoma, high counts of $B7H3^+$ tumor-infiltrating lymphocytes (TILs) were associated with high levels of TNFα and IFNγ in the serum [31]. These findings are consistent with a role for sB7H3 in the differentiation/activation of M1 macrophages.

The association of sB7H3 levels with the progression of IPF patients may be due to the enhanced pulmonary inflammation with increased recruitment of MDSCs plus its expansion in the BM. These findings are consistent with a potential role for sB7H3 in acute exacerbation wherein inflammation and inflammatory cytokine expression are observed in the lungs [5,21,32,33]. Such a role is consistent with that in other chronic inflammatory diseases wherein B7H3 is implicated in the pathogenesis of asthma, autoimmune encephalomyelitis, collagen-induced arthritis, and allergic conjunctivitis [27,34,35]. In this study, higher levels of plasma sB7H3 were correlated with lung function deterioration.

The level of plasma sB7H3 was related to the immunosuppressive status of IPF patients, based on the increased numbers of MDSCs. Recent studies showed that elevated expression of B7H3 in some cancer cells was associated with tumor progression by virtue of its function as an immune checkpoint molecule [10,36–38]. Moreover, a positive correlation between MDSCs and Tregs [39] further suggests that the immunosuppressive effect of sB7H3 may be related to its effects on MDSCs, especially since a positive association between the level of B7H3 expression and the intensity of Treg infiltration has been reported [40]. B7H3 also inhibits human T-cell responses [41] and Th2 activation in murine models [27,34]. However, the significance of these 'suppressor' cells *vis-à-vis* pathogenesis in IPF or its acute exacerbation is unclear, and in some ways antithetical to the observation of heightened innate immune response in the latter case. Tregs or MDSCs are increased in the peripheral blood of IPF patients and correlated with disease progression or disease status [9,39]. Both innate and adaptive immune systems can secrete pro-inflammatory or pro-fibrotic mediators to participate in the initiation and progression of IPF [42]. The potential of MDSCs may rest primarily on their known ability to elaborate and release pro-fibrogenic factors, such as TGFβ [43]. Interestingly, TGFβ treatment itself upregulated B7H3 expression in fibroblasts, which could contribute to the noted increased lung expression of B7H3 in BLM-induced pulmonary fibrosis. Further studies are needed to elucidate the mechanisms underlying the roles of B7H3, MDSCs, and Tregs in IPF pathogenesis and its exacerbation. In addition, studies using a different cohort of IPF patients with/without exacerbation may be helpful in validating the significance of B7H3 in IPF exacerbation as suggested by our findings.

TLT-2 (TREML2) was suggested as a possible receptor for mouse B7H3. Consistent with such a possibility, in this study neutralizing antibodies to TLT-2 abolished the chemotactic activity of sB7H3 on MDSCs. Furthermore, this finding implicated TLT-2 in the overall mechanism by which sB7H3 promoted the recruitment of immune and inflammatory cells. Further *in vivo* research is needed to explore the role of TLT-2 in mediating the effects of sB7H3 in the pathophysiology of IPF and its acute exacerbation.

Acknowledgements

This study was supported by NIH grants HL112880, HL138417, and HL143339. We thank Peking Union

Medical College Hospital, the Chinese Academy of Medical Sciences, and Peking Union Medical College for sponsorship of the scholarship from the China Scholarship Council (to CF). We thank Candace Flaherty and Christi Getty for their assistance in the recruitment of human subjects for collection of peripheral blood samples. We acknowledge the excellent technical assistance of Lisa Riggs for lung tissue section preparation and the H&E staining.

Author contributions statement

SHP and TL conceived the project. KF recruited the human subjects and provided patient demographics plus clinical advice. CF, SHP and TL designed the experiments. CF, AER, JW and TL performed the experiments. CF, SHP and TL analyzed data and wrote the manuscript, which was reviewed by all the authors.

References

1. The Idiopathic Pulmonary Fibrosis Clinical Research Network, Raghu G, Anstrom KJ, *et al*. Prednisone, azathioprine, and *N*-acetylcysteine for pulmonary fibrosis. *N Engl J Med* 2012; **366:** 1968–1977.
2. Raghu G. Idiopathic pulmonary fibrosis: new evidence and an improved standard of care in 2012. *Lancet* 2012; **380:** 699–701.
3. Magnini D, Montemurro G, Iovene B, *et al*. Idiopathic pulmonary fibrosis: molecular endotypes of fibrosis stratifying existing and emerging therapies. *Respiration* 2017; **93:** 379–395.
4. Fernandez IE, Kass DJ. Do circulating monocytes promote and predict idiopathic pulmonary fibrosis progression? *Am J Respir Crit Care Med* 2021; **204:** 9–11.
5. Balestro E, Calabrese F, Turato G, *et al*. Immune inflammation and disease progression in idiopathic pulmonary fibrosis. *PLoS One* 2016; **11:** e0154516.
6. Ashitani J, Mukae H, Taniguchi H, *et al*. Granulocyte-colony stimulating factor levels in bronchoalveolar lavage fluid from patients with idiopathic pulmonary fibrosis. *Thorax* 1999; **54:** 1015–1020.
7. Kreuter M, Lee JS, Tzouvelekis A, *et al*. Monocyte count as a prognostic biomarker in patients with idiopathic pulmonary fibrosis. *Am J Respir Crit Care Med* 2021; **204:** 74–81.
8. Homolka J, Ziegenhagen MW, Gaede KI, *et al*. Systemic immune cell activation in a subgroup of patients with idiopathic pulmonary fibrosis. *Respiration* 2003; **70:** 262–269.
9. Reilkoff RA, Peng H, Murray LA, *et al*. Semaphorin $7a^+$ regulatory T cells are associated with progressive idiopathic pulmonary fibrosis and are implicated in transforming growth factor-β1-induced pulmonary fibrosis. *Am J Respir Crit Care Med* 2013; **187:** 180–188.
10. Yang S, Wei W, Zhao Q. B7-H3, a checkpoint molecule, as a target for cancer immunotherapy. *Int J Biol Sci* 2020; **16:** 1767–1773.
11. Zhang G, Hou J, Shi J, *et al*. Soluble CD276 (B7-H3) is released from monocytes, dendritic cells and activated T cells and is detectable in normal human serum. *Immunology* 2008; **123:** 538–546.
12. Greenwald RJ, Freeman GJ, Sharpe AH. The B7 family revisited. *Annu Rev Immunol* 2005; **23:** 515–548.
13. Zhang SS, Tang J, Yu SY, *et al*. Expression levels of B7-H3 and TLT-2 in human oral squamous cell carcinoma. *Oncol Lett* 2015; **10:** 1063–1068.
14. Stanciu LA, Bellettato CM, Laza-Stanca V, *et al*. Expression of programmed death-1 ligand (PD-L) 1, PD-L2, B7-H3, and inducible costimulator ligand on human respiratory tract epithelial cells and regulation by respiratory syncytial virus and type 1 and 2 cytokines. *J Infect Dis* 2006; **193:** 404–412.
15. Suh WK, Wang SX, Jheon AH, *et al*. The immune regulatory protein B7-H3 promotes osteoblast differentiation and bone mineralization. *Proc Natl Acad Sci U S A* 2004; **101:** 12969–12973.
16. Hashiguchi M, Kobori H, Ritprajak P, *et al*. Triggering receptor expressed on myeloid cell-like transcript 2 (TLT-2) is a counter-receptor for B7-H3 and enhances T cell responses. *Proc Natl Acad Sci U S A* 2008; **105:** 10495–10500.
17. Inamura K, Amori G, Yuasa T, *et al*. Relationship of B7-H3 expression in tumor cells and tumor vasculature with FOXP3+ regulatory T cells in renal cell carcinoma. *Cancer Manag Res* 2019; **11:** 7021–7030.
18. Chen L, Zhang G, Sheng S, *et al*. Upregulation of soluble B7-H3 in NSCLC-derived malignant pleural effusion: a potential diagnostic biomarker correlated with NSCLC staging. *Clin Chim Acta* 2016; **457:** 81–85.
19. Zhang X, Zhao X, Sun H, *et al*. The role of miR-29c/B7-H3 axis in children with allergic asthma. *J Transl Med* 2018; **16:** 218.
20. Yoon BR, Chung YH, Yoo SJ, *et al*. Preferential induction of the T cell auxiliary signaling molecule B7-H3 on synovial monocytes in rheumatoid arthritis. *J Biol Chem* 2016; **291:** 4048–4057.
21. Nakashima T, Liu T, Hu B, *et al*. Role of B7H3/IL-33 signaling in pulmonary fibrosis-induced profibrogenic alterations in bone marrow. *Am J Respir Crit Care Med* 2019; **200:** 1032–1044.
22. Raghu G, Remy-Jardin M, Myers JL, *et al*. Diagnosis of idiopathic pulmonary fibrosis. An official ATS/ERS/JRS/ALAT clinical practice guideline. *Am J Respir Crit Care Med* 2018; **198:** e44–e68.
23. Hashimoto N, Jin H, Liu T, *et al*. Bone marrow-derived progenitor cells in pulmonary fibrosis. *J Clin Invest* 2004; **113:** 243–252.
24. Liu T, Baek HA, Yu H, *et al*. FIZZ2/RELM-β induction and role in pulmonary fibrosis. *J Immunol* 2011; **187:** 450–461.
25. Livak KJ, Schmittgen TD. Analysis of relative gene expression data using real-time quantitative PCR and the 2(−Delta Delta C(T)) method. *Methods* 2001; **25:** 402–408.
26. Ding L, Liu T, Wu Z, *et al*. Bone marrow $CD11c^+$ cell-derived amphiregulin promotes pulmonary fibrosis. *J Immunol* 2016; **197:** 303–312.
27. Luo L, Zhu G, Xu H, *et al*. B7-H3 promotes pathogenesis of autoimmune disease and inflammation by regulating the activity of different T cell subsets. *PLoS One* 2015; **10:** e0130126.
28. Janick-Buckner D, Ranges GE, Hacker MP. Alteration of bronchoalveolar lavage cell populations following bleomycin treatment in mice. *Toxicol Appl Pharmacol* 1989; **100:** 465–473.
29. Moore BB, Hogaboam CM. Murine models of pulmonary fibrosis. *Am J Physiol Lung Cell Mol Physiol* 2008; **294:** L152–L160.
30. Chen X, Li Y, Blankson S, *et al*. B7-H3 augments inflammatory responses and exacerbates brain damage via amplifying NF-κB p65 and MAPK p38 activation during experimental pneumococcal meningitis. *PLoS One* 2017; **12:** e0171146.
31. Iida K, Miyake M, Onishi K, *et al*. Prognostic impact of tumor-infiltrating CD276/Foxp3-positive lymphocytes and associated circulating cytokines in patients undergoing radical nephrectomy for localized renal cell carcinoma. *Oncol Lett* 2019; **17:** 4004–4010.
32. Emura I, Usuda H. Acute exacerbation of IPF has systemic consequences with multiple organ injury, with SRA^+ and $TNF\text{-}\alpha^+$ cells in the systemic circulation playing central roles in multiple organ injury. *BMC Pulm Med* 2016; **16:** 138.
33. Schupp JC, Binder H, Jäger B, *et al*. Macrophage activation in acute exacerbation of idiopathic pulmonary fibrosis. *PLoS One* 2015; **10:** e0116775.
34. Fukushima A, Sumi T, Fukuda K, *et al*. B7-H3 regulates the development of experimental allergic conjunctivitis in mice. *Immunol Lett* 2007; **113:** 52–57.
35. Gu W, Zhang X, Yan Y, *et al*. B7-H3 participates in the development of asthma by augmentation of the inflammatory response independent of TLR2 pathway. *Sci Rep* 2017; **7:** 40398.

36. Altan M, Pelekanou V, Schalper KA, *et al*. B7-H3 expression in NSCLC and its association with B7-H4, PD-L1 and tumor-infiltrating lymphocytes. *Clin Cancer Res* 2017; **23:** 5202–5209.
37. Benzon B, Zhao SG, Haffner MC, *et al*. Correlation of B7-H3 with androgen receptor, immune pathways and poor outcome in prostate cancer: an expression-based analysis. *Prostate Cancer Prostatic Dis* 2017; **20:** 28–35.
38. Chen JT, Chen CH, Ku KL, *et al*. Glycoprotein B7-H3 overexpression and aberrant glycosylation in oral cancer and immune response. *Proc Natl Acad Sci U S A* 2015; **112:** 13057–13062.
39. Fernandez IE, Greiffo FR, Frankenberger M, *et al*. Peripheral blood myeloid-derived suppressor cells reflect disease status in idiopathic pulmonary fibrosis. *Eur Respir J* 2016; **48:** 1171–1183.
40. Wang L, Cao NN, Wang S, *et al*. Roles of coinhibitory molecules B7-H3 and B7-H4 in esophageal squamous cell carcinoma. *Tumour Biol* 2016; **37:** 2961–2971.
41. Leitner J, Klauser C, Pickl WF, *et al*. B7-H3 is a potent inhibitor of human T-cell activation: no evidence for B7-H3 and TREML2 interaction. *Eur J Immunol* 2009; **39:** 1754–1764.
42. Wynn TA. Integrating mechanisms of pulmonary fibrosis. *J Exp Med* 2011; **208:** 1339–1350.
43. Sanaei MJ, Salimzadeh L, Bagheri N. Crosstalk between myeloid-derived suppressor cells and the immune system in prostate cancer: MDSCs and immune system in prostate cancer. *J Leukoc Biol* 2020; **107:** 43–56.

SUPPLEMENTARY MATERIAL ONLINE

Figure S1. Evaluation of mouse lung fibrosis using Masson's trichrome staining